Pickup protons: Comparisons using the three-dimensional MHD HHMS-PI model and Ulysses SWICS measurements

Devrie S. Intriligator,[1] Thomas Detman,[1] George Gloecker,[2] Christine Gloeckler,[2] Murray Dryer,[1] Wei Sun,[1] James Intriligator,[1,3] and Charles Deehr[4]

Received 30 November 2011; revised 27 March 2012; accepted 27 April 2012; published 12 June 2012.

[1] We report the first comparisons of pickup proton simulation results with in situ measurements of pickup protons obtained by the SWICS instrument on Ulysses. Simulations were run using the three dimensional (3D) time-dependent Hybrid Heliospheric Modeling System with Pickup Protons (HHMS-PI). HHMS-PI is an MHD solar wind model, expanded to include the basic physics of pickup protons from neutral hydrogen that drifts into the heliosphere from the local interstellar medium. We use the same model and input data developed by Detman et al. (2011) to now investigate the pickup protons. The simulated interval of 82 days in 2003–2004, includes both quiet solar wind (SW) and also the October–November 2003 solar events (the "Halloween 2003" solar storms). The HHMS-PI pickup proton simulations generally agree with the SWICS measurements and the HHMS-PI simulated solar wind generally agrees with SWOOPS (also on Ulysses) measurements. Many specific features in the observations are well represented by the model. We simulated twenty specific solar events associated with the Halloween 2003 storm. We give the specific values of the solar input parameters for the HHMS-PI simulations that provide the best combined agreement in the times of arrival of the solar-generated shocks at both ACE and Ulysses. We show graphical comparisons of simulated and observed parameters, and we give quantitative measures of the agreement of simulated with observed parameters. We suggest that some of the variations in the pickup proton density during the Halloween 2003 solar events may be attributed to depletion of the inflowing local interstellar medium (LISM) neutral hydrogen (H) caused by its increased conversion to pickup protons in the immediately preceding shock.

Citation: Intriligator, D. S., T. Detman, G. Gloecker, C. Gloeckler, M. Dryer, W. Sun, J. Intriligator, and C. Deehr (2012), Pickup protons: Comparisons using the three-dimensional MHD HHMS-PI model and Ulysses SWICS measurements, *J. Geophys. Res.*, *117*, A06104, doi:10.1029/2011JA017424.

1. Introduction

[2] The specific focus of this paper is the HHMS-PI simulation [*Detman et al.*, 2011] of the pickup proton parameters at Ulysses and their comparison with the Ulysses SWICS measurements [*Gloeckler et al.*, 1992, 1993, 1994]. Pickup ions (mostly protons) play many key roles in the heliosphere. Pickup protons come from LISM neutral H that drifts into the heliosphere due to the motion of the Sun through the LISM. As it approaches the Sun, neutral H is ionized by two processes: photoionization and charge exchange with SW protons. Upon ionization, these protons are immediately "picked up" by the SW magnetic field. Due to the high relative velocity of the incoming neutral H with respect to the solar wind, the pickup process transfers significant energy and momentum to the SW. The SW protons neutralized by charge exchange become energetic neutral atoms (ENAs) and are lost from the SW. Out in the LISM ENAs have the possibility to charge exchange again, with interstellar protons, but that process is beyond the scope of this paper. Early observations of pickup ions were made by *Möbius et al.* [1985], *Gloeckler et al.* [1993, 1994], and *Intriligator et al.* [1996]. Gloeckler, Geiss, and colleagues have since published many important results based on their analyses of Ulysses SWICS data. Möbius and colleagues have described other significant aspects of pickup ion data.

[3] *Whang* [1998] provided a strong theoretical foundation for the study of pickup ions in the heliosphere. *Wang et al.* [2000] described and gave results from a one-dimensional,

[1]Space Plasma Laboratory, Carmel Research Center, Inc., Santa Monica, California, USA.
[2]Atmospheric, Oceanic and Space Sciences, University of Michigan, Ann Arbor, Michigan, USA.
[3]School of Psychology, Bangor University, Bangor, UK.
[4]Geophysical Institute, University of Alaska Fairbanks, Fairbanks, Alaska, USA.

Corresponding author: D. S. Intriligator, Space Plasma Laboratory, Carmel Research Center, Inc., PO Box 1732, Santa Monica, CA 90406, USA. (devriei@aol.com)

time-dependent, MHD solar wind model with pickup protons. Their model has a time-dependent lower boundary condition at 1 AU driven by SW observations from ACE. *Usmanov and Goldstein* [2006] incorporated the physics of pickup protons into their existing three-dimensional, steady state, region III, solar wind (SW) model. Its boundary conditions are given by their region II model; their region I model begins at the photosphere.

[4] The key feature of both the Hybrid Heliospheric Modeling System (HHMS) [*Detman et al.*, 2006], and the new model Hybrid Heliospheric Modeling System with Pickup Protons (HHMS-PI) [*Detman et al.*, 2011] is that they are 3D, time-dependent models that have the lower boundaries of their MHD SW models at 0.1 AU. They circumvent the computationally intense and demanding MHD modeling of the solar corona by using the Wang-Sheeley-Arge (WSA) source surface current-sheet model [*Arge and Pizzo*, 2000] in combination with an empirical interface module that translates source-surface map outputs into MHD boundary conditions. Hence the word "hybrid" in the name.

[5] Our goal in this work is to test and improve our understanding of pickup protons throughout the heliosphere out to the outer heliosphere by simulating multiple spacecraft observations as accurately as we can, and by so doing, putting the various spacecraft observations into a large scale 3D, time-dependent context. To do this, we did two types of parameter tuning. We tuned parameters in the empirical interface boundary condition (BC) module to bring the HHMS-PI simulated, quiet background, SW at Earth into agreement with ACE observations [*Detman et al.*, 2011]. We also tuned HHMS-PI shock input parameters, first to obtain agreement between simulated shock arrival times and strengths with ACE; and in a second phase, to achieve agreement with both ACE and Ulysses parameters and onsets/magnitudes of events. In regard to our use of parameter tuning, we reiterate that we are simulating spacecraft observations, not predicting, and that successful simulation often precedes successful prediction. In addition, successful tuning can lead to important knowledge of the relative significance of various input (tuning) parameters. While we are not predicting specific parameters at ACE and Ulysses, HHMS-PI does tell us what the global configuration of the heliosphere was at that time. For example, it gives us the pickup proton and solar wind characteristics not just where observations were made, but everywhere from close to the Sun to the observer. This global context of the single point spacecraft measurement is very important for many studies.

[6] The success of such tuning efforts can only be achieved, and measured, by the use of quantitative verification. We stress the importance of quantitative verification, "benchmarking," in this case, the HHMS-PI results are compared with the pickup proton measurements from the SWICS instrument, and SW measurements from the SWOOPS instrument on the Ulysses spacecraft, near 5.2 AU from the Sun. Details are given below. The simulation results reported here cover the interval from 2003 October 12 to 2004 January 02. This ~82-day time interval at Ulysses includes both quiet SW and the October–November 2003 solar events, also known as the "Halloween 2003" solar events. The verification, or benchmarking, numbers shown on the figures are for the 60-day time interval covered by the plot. But here, we also must caution the reader that such numbers can be highly sensitive to the choice of the interval for which they are calculated.

[7] In the next section we describe some aspects of HHMS-PI. The section after that describes the benchmarking of HHMS-PI pickup proton simulations at Ulysses through comparisons of the HHMS-PI simulation results with the in situ SWICS pickup proton measurements on Ulysses, and SWOOPS SW measurements. Then the SWICS measurements are described. The last section is the Discussion.

2. HHMS-PI: Incorporation of Pickup Protons in the Time Dependent 3D MHD HHMS

[8] We are using HHMS-PI as an after the fact simulation tool, not for predictions. HHMS [*Detman et al.*, 2006] is a 3D, time-dependent, ideal magnetohydrodynamic (MHD), numerical solar wind model that is driven by solar observations; it solves eight simultaneous partial differential equations: three for momentum, three for field components, one for mass conservation, and one for energy. In converting it into HHMS-PI [*Detman et al.*, 2011], two more equations were added to the system, one for pickup proton density and one for pickup proton pressure. HHMS-PI is thus a two-fluid model in which the two fluids share a common velocity vector. The equations are solved in conservation form, so the model is "shock capturing." The full set of ten equations solved by HHMS-PI can be described by a single vector equation, in spherical coordinates, (r, θ, ϕ):

$$\frac{\partial \mathbf{U}}{\partial t}+\frac{\partial \mathbf{F}}{\partial r}+\frac{1}{r\sin\theta}\frac{\partial \mathbf{G}}{\partial \theta}+\frac{1}{r\sin\theta}\frac{\partial \mathbf{H}}{\partial \phi}=\mathbf{S}, \tag{1}$$

where **U** is a vector of flow variables; **F**, **G**, **H** are vectors of fluxes in the (r, θ, ϕ) directions respectively, and **S** is a vector of source terms.

[9] In HHMS-PI, the transfers of mass, energy, and momentum associated with pickup protons are represented by source terms in the conservation equations, i.e., by terms in the **S** vector. We generally followed the approach taken *by Usmanov and Goldstein* [2006] (UG), in the modification of our governing MHD equations to include pickup protons. Much of the pickup proton physics is represented by source terms, in the vector. Here, we also mainly followed UG. We departed from UG on the form of the neutral H density. The steady state thermal conduction problem (Alfven wave damping, turbulence, etc.) is still being investigated [e.g., *Usmanov and Goldstein*, 2006], but not in time-dependent models. This theoretical problem is beyond our scope. In our time-dependent methodology we have chosen to use the polytrope to mimic this question for both the SW and the pickup protons.

[10] The UG region III model goes from 1 to 100 AU; they took the neutral H density to be uniform in that range, with $N_H = 0.1$ cm^{-3}. Since our lower boundary is at 0.1 AU, we instead, adopted the distribution used by *Wang et al.* [2000], given below in this section, which also has $N_H = 0.1$ cm^{-3} at infinity, but which goes to zero at the Sun. The key factors in the source terms are the pickup proton production rates by photoionization and by charge exchange. The photoionization production rate is given by, $q_{ph} = \nu(r_o^2/r^2)N_H$, where ν is

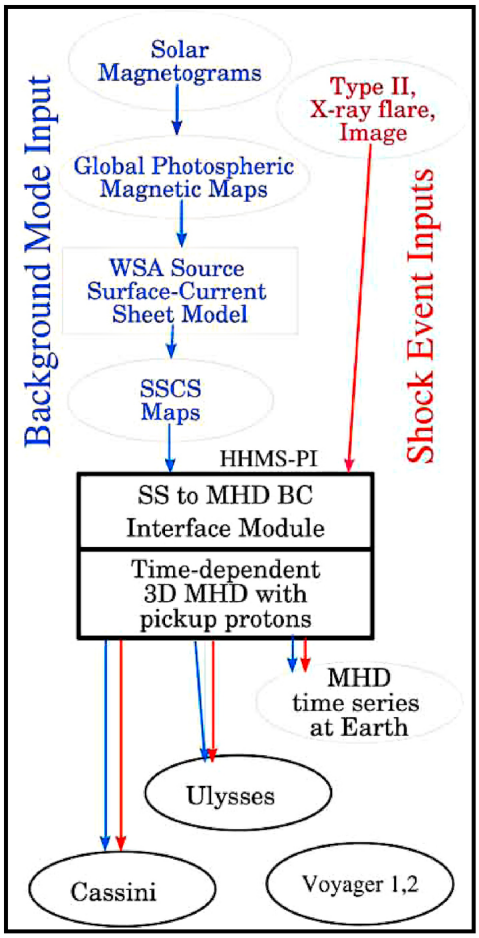

Figure 1. Schematic showing the two input tracks in the full 3D MHD HHMS-PI. Continuous inputs of solar parameters are input into both the background solar wind track on the left and the solar transient track on the right, as discussed in some detail in the text. The content of this figure is the same as in Figure 1 in *Detman et al.* [2011].

the rate of photoionization per H atom at the distance r_o; $\nu = 9 \times 10^{-8} s^{-1}$ for $r_o = 1$ AU. The production rate by charge exchange is: $q_{ex} = \sigma N_S N_H |\Delta V|$, where $\sigma = 2 \times 10^{-15}$ cm^2 is the mean charge exchange cross section of H, the solar wind density is N_S; N_H is the neutral H density, and $|\Delta V|$ is the relative velocity between the neutral H and the solar wind. The actual neutral H density and distribution function in the heliosphere depend on the inflow speed, direction, and temperature of neutral H in the upstream LISM, but the distribution function also evolves via its interaction with the SW and so depends strongly on location within the heliosphere [*Whang*, 1998]. However, for this initial modeling effort, we adopted the stationary, cold (zero velocity), and spherically symmetric distribution given by *Wang et al.* [2000]: $N_H(r) = N_H(\infty)\ e^{-\lambda/r}$, where $N_H(\infty) = 0.1$, and $\lambda = 4$ AU. In this case, the $|\Delta V|$ in the charge exchange source term reverts to just the SW speed. Also note this simplified treatment is not mass conserving, production of pickup protons is not balanced by a loss of neutral H. While this stationary, spherically symmetric, zero velocity neutral H model is necessary for a steady state model such as *Usmanov and Goldstein* [2006] and appropriate for the 1D model of *Wang et al.* [2000], we consider it to be only a starting point. The question arises, how do the simplifications of this neutral H model impact results? We address this question below. We plan to implement more realistic (nonzero velocity, mass conserving) models for N_H in future work.

[11] Good model results depend critically on the appropriate physics included in the model for the problem, as discussed above for the HHMS-PI model, and on good inputs to the model. Accordingly, we devoted considerable attention to our time-dependent boundary conditions. The SW model in HHMS-PI, like HHMS, has its lower boundary at 0.1 AU. Details of the solar-corona events that launch shock waves into the solar wind are not well observed. Thus, first-guess model inputs to simulate these events were inferred from available observations such as solar images, GOES X-ray flare intensity and duration, CME images, and Type II radio bursts. We then used an iterative shock strength "tuning" process to bring the HHMS-PI simulated shock strengths and arrival times at Earth into close agreement with SW observations from the NASA Advanced Composition Explorer (ACE) spacecraft. We then extended the model grid to 5.5 AU and compared the model results with observations from the Ulysses spacecraft, including both SW data from the SWOOPS instrument and pickup proton data from the SWICS instrument. We then undertook a more difficult "bi-tuning" process, to get agreement between simulated and observed shocks at both ACE and Ulysses. This bi-tuning process primarily involved [*Detman et al.*, 2011] a somewhat trial and error series of iterations adjusting, for example, the heliolongitude (lon), disturbance radius (rad), and the shock speed (shSpd). The results of this bi-tuning process are discussed below.

[12] HHMS-PI has two input tracks that are illustrated in Figure 1. Figure 1 here is identical in content to Figure 1 in *Detman et al.* [2011]. The first track on the left side in Figure 1, gives the quiet, inhomogeneous, and slowly changing, (background) SW including the interplanetary magnetic field (IMF) with its sector structure, and co-rotating interaction regions (CIRs). The lower boundary condition of the MHD solar wind model in HHMS-PI is driven indirectly by the Wang-Sheeley-Arge (WSA) source surface (SS) current-sheet (CS) model [*Arge and Pizzo*, 2000]. That is, it is driven via an empirical interface module that converts source surface map parameters, into MHD parameters at 0.1 AU, the height of the lower grid boundary [*Detman et al.*, 2006]. The WSA model is a steady state model of the solar corona. It produces global maps of the magnetic field, and other topological characteristics of the field at the top of the corona (the source surface). In the WSA model the SS is at a height of 2.5 solar radii, but with the added current-sheet, output maps give conditions at a height of 5 solar radii. Although not officially "operational," the WSA model has been in routine daily operation at the NOAA Space Weather Prediction Center, for more than a decade. The SS maps used in this study came from ftp://helios.sec.noaa.gov/pub/lmayer/WSA/full_fits_ss_maps/MWO/. We used "full rotation" maps. The interval between these maps is the Carrington rotation period, 27.2753 days. However, since the input to the WSA model consists of daily solar magnetograms over a solar rotation, combined into a

Table 1. Shock Parameters After Adjusting for Time of Arrival at Both ACE and Ulysses[a]

Date	Time	DOY	Latitude	Longitude	Rad	shSpd	Tau	FF
2003-10-19	16:50	(292.701)	5	−56.0	102.0	519.6	1.33	507
2003-10-21	03:47	(294.158)	−10	−90.0	100.0	517.0	0.67	508
2003-10-22	09:38	(295.401)	−2	−22.0	100.0	781.5	3.00	509
2003-10-23	08:27	(296.352)	−21	−88.0	108.0	1276.0	1.50	510
2003-10-25	04:15	(298.177)	−15	−43.0	120.0	530.0	2.00	511
2003-10-26	06:17	(299.262)	−18	−43.0	120.0	574.1	3.00	512
2003-10-26	17:35	(299.733)	5	32.6	70.2	1027.0	3.50	513
2003-10-28	11:02	(301.460)	−16	−8.0	120.0	1951.0	3.00	514
2003-10-29	20:44	(302.864)	−14	1.0	123.0	1612.4	1.50	515
2003-11-01	22:34	(305.940)	−10	61.0	120.0	820.9	1.00	516
2003-11-02	17:14	(306.718)	−14	82.5	158.0	1791.4	1.00	517
2003-11-03	01:24	(307.058)	10	85.0	100.0	725.0	1.75	518
2003-11-03	09:56	(307.414)	8	77.0	120.0	1131.3	1.50	519
2003-11-04	19:43	(308.822)	−19	78.8	102.0	1580.7	1.50	520
2003-11-07	15:54	(311.663)	−18	120.0	100.0	1682.7	2.00	520.2
2003-11-11	13:35	(315.566)	−3	88.8	93.7	807.0	3.00	521
2003-11-13	09:24	(317.392)	1	−90.0	101.0	718.5	3.00	522
2003-11-17	09:17	(321.387)	−1	−33.0	100.0	547.0	2.00	523
2003-11-18	07:47	(322.324)	0	−18.0	221.1	918.4	3.00	524
2003-11-20	07:47	(324.324)	1	14.0	104.9	997.9	0.75	525

[a]Date, Time, Day of Year: start time of metric Type II. Latitude (degrees), Longitude (degrees), Rad: width of shock (degrees). shSpd is Vs (km/s): shock speed input at the Sun from real-time radio and halo/partial halo CME plane-of-sky speed estimates. Tau (hrs): coronal shocks piston driving time above flare site. FF#: real-time "fearless forecast" events. As discussed in the text, the content of this table is essentially the same as Table 3 in *Detman et al.* [2011].

global magnetic map of the photosphere, the resulting SS maps have an effective update interval of about a day. We use two consecutive SS maps to generate time-dependent boundary conditions. The interface module in Figure 1 uses a set of empirical formulas to translate SS map parameters into MHD boundary conditions. The model captures the buildup of CIRs. Transient events (on the right in Figure 1) are superimposed on this background activity.

[13] The second input track, on the right side in Figure 1, introduces perturbations for shocks due to specific solar events: such as CMEs, flares, etc., based on their specific location (longitude, latitude) on the Sun; the type (optical, x-ray, etc.); the width of the initiating disturbance; its duration; shock speed, etc. The specific parameters we used in the present study, for the Halloween 2003 solar events, are given in Table 3 of *Detman et al.* [2011] and Table 1 here. We note that the content of Table 1 here is the same as the content of Table 3 in *Detman et al.* [2011] with two exceptions. (1) The tau data values in Table 1 here are shown to the second decimal place whereas they are shown to the first decimal place in Table 3 in *Detman et al.* [2011]. (2) In the last column of Table 1 here we list the backside solar event as 520.2 whereas it's listed in Table 3 of *Detman et al.* [2011] as a second "520" even though the *Detman et al.* [2011, paragraph 34] text says: "we added the event listed as FF 520.2 in the first column of Table 3." As discussed in *Detman et al.* [2011, paragraph 34], this is an important addition to the FF list. In the bi-tuning process – where we matched the shock arrivals at both ACE and Ulysses – we could not reproduce the high solar wind speeds seen at Ulysses near Day 320 using only the original FF events. As stated in *Detman et al.* [2011, paragraph 34],

> …*de Koning et al.* [2005] indicated the occurrence of an unusually fast CME originating from beyond the visible disk of the Sun on 7 November at 1554 UT. On the basis of that information, we added the event listed as FF 520.2 in the first column of Table 3. A longitude of W120, and latitude of S18 is consistent with this event coming from the same active region (NOAA/ SWPC AR 10486) that produced FF520, FF517, and/or FF514. When we added this event to our shock inputs and adjusted the shock speed to make the simulated shock arrive at day 318.984, we got a significantly better match to Ulysses velocities around that time, but we also got a greatly improved match with a reverse shock at Ulysses near day 320, that produced the highest speeds at Ulysses in the study interval.

[14] Both the background mode tuning and the shock input tuning done to match simulated to the observed shock arrivals at both ACE and Ulysses are described in more detail in *Detman et al.* [2011]. A comparison of the specific parameters in Table 1 here with the corresponding parameters in Tables 1 and 2 in *Detman et al.* [2011] indicates the input parameter variations that were implemented in the tuning of the data for these specific events for the ACE tuning and the bi-tuning with ACE and Ulysses. These comparisons show that a few changes were made in the latitude locations (lat) of the solar events, more changes were made in the longitude locations (lon) of the solar events, and the most changes were made in the shock speed (shSpd) of the solar events. Also as part of the iterative bi-tuning process changes were made in the disturbance radius on the Sun (rad). The first two tuning parameters (i.e., "lat" and "lon") are associated with the specific locations of the solar events on the solar surface, and the shock speed "shSpd" is associated with the initial speed of the event as it leaves the solar surface. "Rad" is associated with the shock input radius, i.e., the width of the solar event as it leaves the Sun. These comparisons of the specific changes between Tables 1, 2, and 3 in *Detman et al.* [2011] and between Tables 1 and 2 in *Detman et al.* [2011] and Table 1 in the present paper (which has the same content as Table 3 in *Detman et al.* [2011]) and also the examination of the content of Table 1 here all show that the tuning and bi-tuning changes and values are realistic properties associated with the solar surface (i.e., the location of the events) and/or with the physical properties of the initiation of the events (i.e., the

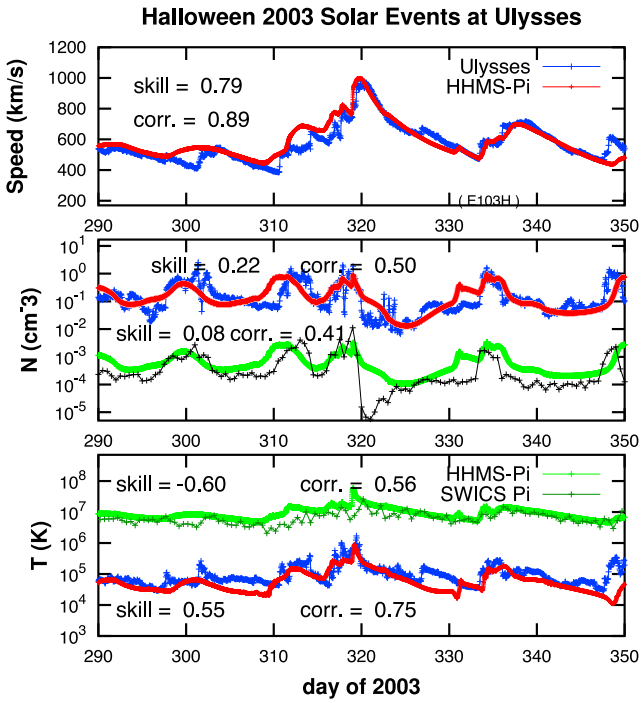

Figure 2. Benchmarking HHMS-PI simulations for solar wind and pickup protons at Ulysses for 60 days in 2003 including quiescent "quiet" undisturbed times and the "disturbed" times associated with the Halloween 2003 events. Also shown are the HHMS-PI simulation comparisons at Ulysses with SWOOPS solar wind speed, solar wind proton density, and solar wind temperature; and with SWICS pickup proton density and pick-up proton temperature for the "quiet" solar wind both before and after the Halloween events and for the Halloween 2003 events. Note the generally good agreement between the HHMS-PI simulations (in red for the solar wind proton parameters and in green for the pickup proton parameters) and the measured plasma speed, densities, and temperatures for both the solar wind protons (in blue) and the measured SWICS pickup proton density and temperature parameters (in gray) even though at times during the Halloween 2003 event the shape of the plasma distributions is varying greatly as illustrated in the SWICS spectra (e.g., Days 319.5–320.5) in Figure 3. See text for possible explanations for the *increased* pickup proton density differences between SWICS and HHMS-PI following Day 320.

initial shock speeds (shSpd) and widths of the initial disturbances (rad)). Thus, they along with the HHMS-PI results presented in *Detman et al.* [2011] and the results presented here in the present paper are a confirmation that the HHMS-PI model effort is worthwhile.

3. Comparisons Between HHMS-PI Simulated Parameters and Parameters Derived From Ulysses SWICS Measurements

[15] An important demonstration of the HHMS-PI's robustness is shown in Figure 2 where the comparisons between the HHMS-PI simulations and the measured Ulysses data for the time interval from Day 290 to 350, 2003 are presented. The Ulysses SWICS instrument and measurements have been described in detail in many papers including *Gloeckler et al.*, 1992, 1993, 1994. The SWICS data used in our comparisons are standard Ulysses SWICS data and are described in the SWICS papers referenced above. Figure 2 (top) shows the high correlation coefficient (rc = ~0.9) for the simulated SW speed with the measured SWOOPS SW speed. This good agreement shows the success of our shock input tuning process and our background mode parameter tuning. Figure 2 indicates the relatively good agreement of the HHMS-PI pickup proton density simulation (middle panel) and temperature simulation (lower panel) that was achieved with the Ulysses SWICS data for both the quiescent SW and for the complex and challenging Halloween 2003 events.

[16] Each of the simulated parameters shown in Figure 2 was verified against the corresponding observation using two well-known metrics: skill score and correlation coefficient, both are printed in Figure 2 for each parameter. Skill score, also known as prediction efficiency, is defined as 1.0 minus the ratio of mean squared error (MSE) to the sample variance (VAR):

$$Skill = PE = 1 - \frac{MSE}{VAR},$$

where

$$MSE = 1/N \sum (f_i - x_i)^2 \text{ and } VAR = 1/N \sum (\bar{x} - x_i)^2.$$

Perfect, and only perfect, predictions give a skill score, or PE, equal to 1.0. The correlation coefficient is given by

$$rc = \frac{\sum (f_i - \bar{f})(x_i - \bar{x})}{\left[\sum (f_i - \bar{f})^2 \sum (x_i - \bar{x})^2\right]^{1/2}}.$$

A high correlation coefficient between f and x means that a good prediction of x can be made by a linear transformation of f.

[17] Figure 2 (middle) shows that the simulated to observed correlations (rc's) for both the SW proton density and the pickup proton density are ~0.5 and 0.4, respectively. The pickup proton density (and temperature) shown in Figure 2 were extracted from the distribution function in the following manner: the approximate solar wind frame (w) distribution, f(w) was computed where w = W − 1. The approximate density was then computed by the standard phase-space-integration of the solar wind frame pickup ion spectrum from w = 0.35 to w = 1.1, assuming an isotropic distribution in the solar wind frame. Inspection of Figure 2 indicates that on average the HHMS-PI SW proton densities and pickup proton densities are in agreement with the data. Moreover, the intervals of excursions in the densities are also similar in the model results and in the data. Figure 2 (bottom) shows the results for the temperature comparisons between the HHMS-PI simulations and the measured solar wind proton and pickup proton temperatures. The corresponding correlation coefficients (rc's) are ~0.8 and 0.6, respectively.

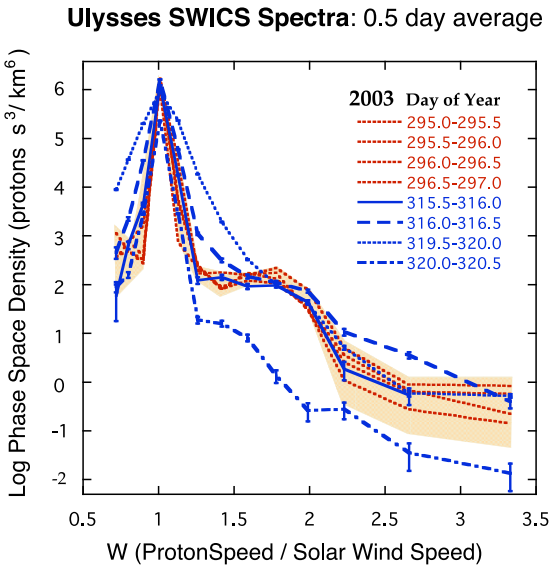

Figure 3. SWICS proton phase space density distributions for eight half-day intervals. Four half-day intervals (Day 295.0–297.0, 2003) are in the quiescent solar wind prior to the Halloween 2003 events, and for four half-day intervals (Day 315.5–320.5, 2003) are in the disturbed solar wind associated with the Halloween 2003 events. The shaded portion envelopes the "quiet" times and the errors, including the Day 315.5–316.0 period. The blue lines show the progression of the data during a disturbance associated with the Halloween events. The proton phase space density distributions are plotted as a function of the ratio of the proton speed to the solar wind He bulk speed. The distributions show three components: (1) the bulk solar wind proton peak centered at W $\sim$ 1, uncorrected for saturation; (2) the interstellar pickup protons in the W range of $\sim$1.4 to $\sim$2.0; and (3) the suprathermal power law tail above W $\sim$ 2. Poor counting statistics in the tail region preclude using a finer W resolution of SWICS. Notice for the more disturbed spectra (Days 319.5 to 320.5) associated with the Halloween 2003 events the more drastic changes in the distributions in terms of both their shapes and the levels of the intensities.

[18] The question raised earlier about our adoption, from *Wang et al.* [2000] of the fixed, spherically symmetric, zero velocity, neutral H density can now be addressed in the context of Figure 2. Figure 2 (middle) shows a deep depletion in the SWICS observed pickup protons on Day 320 immediately following a peak associated with a passing shock. HHMS-PI captured the peak, but not the deep depletion. Instead, the simulated pickup proton density shows mild depletion, similar to the depletion in the simulated SW proton density. We believe the observed depletion of pickup protons may be the result of depleted neutral H caused by its increased conversion to pickup protons in the immediately preceding shock. The product, $N_S N_H |V|$ in the above charge exchange source term q_{ex}, introduces a strongly nonlinear coupling that results in localized high pickup proton densities in SW shocks. The current stationary neutral H model ignores the depletion of neutral H in this process. A reduced neutral H density would reduce the pickup proton production rate. Thus the "miss" of this deep pickup proton depletion event by HHMS-PI demonstrates the case for a more realistic neutral H model, and should be a good test case for such an improvement. Disagreements between the HHMS-PI simulations and the measurements are useful for analyzing simulation inputs, assumptions, modeling, etc. This illustrates how disagreements between the HHMS-PI simulations and the measurements often lead to added insights into the important underlying physical mechanisms.

4. SWICS Phase Space Density Distributions

[19] Figure 3 shows eight SWICS spacecraft frame proton phase space density distributions (see *Gloeckler et al.* [1992] for description of the SWICS instrument on Ulysses) for half-day intervals: four half-day intervals (Days 295.0–297.0, 2003) in the quiescent solar wind prior to, and for four half-day intervals (Day 315.5–320.5, 2003) in the disturbed solar wind associated with the Halloween 2003 events. The shaded portion envelopes the "quiet" times and the errors, including the Day 315.5–316.0 period. The blue lines show the progression of the "disturbed" data during a disturbance associated with the Halloween 2003 events. The proton phase space density distributions are plotted as a function of the ratio (W) of the proton speed to the solar wind He bulk speed. The distributions show three components: (1) the bulk solar wind proton peak centered at W = 1, uncorrected for saturation; (2) the interstellar pickup protons in the W range of $\sim$1.4 to $\sim$2.0; and (3) the suprathermal power law tail above W = 2. Poor counting statistics in the tail region preclude using a finer W resolution of SWICS.

[20] Each of the examples shown in Figure 3 was obtained by averaging over a half-day interval as indicated in the figure. Comparison of the first two "disturbed" pickup proton phase space density distributions from Day 315.5–316.0, 2003 and from Day 316.0–316.5, 2003, respectively, shows that the plasma phase space density distributions are similar but the first distribution has somewhat lower phase space densities at the lowest energy and at the highest energies. In contrast, comparisons of the third and fourth "disturbed" pickup proton phase space density distributions, from Day 319.5–320.0, 2003 and Day 320.0–320.5, 2003, respectively, show a markedly different shape of the two distributions as well as considerably different levels of phase space densities. This change in the pickup proton phase space density distribution near Day 320, 2003 is reflected in the change in the SWICS pickup proton densities in Figure 2. For the more disturbed spectra in Figure 3 (Days 319.5 to 320.5) associated with the Halloween 2003 events there are more drastic changes in the distributions in terms of both their shapes and the levels of the intensities.

5. Discussion

[21] In this paper we focus on the pickup protons and build on the work with our 3D MHD HHMS-PI model in *Detman et al.* [2011]. We have performed HHMS-PI simulations for more than 80 days: October 12, 2003 to January 2, 2004. This time interval includes both quiet intervals and the October–November 2003 (Halloween 2003) events. Figure 2 showed that generally there was good agreement between the HHMS-PI modeled pickup proton densities and

temperatures and the SWICS measured pickup proton densities and temperatures on Ulysses near 5.2 AU for both the quiescent SW intervals and for the Halloween 2003 solar events. We believe that when we model less complex solar events and more isolated solar events, there will be even better agreement between the HHMS-PI modeled results for pickup proton density and temperature and the measured SWICS pickup proton densities and temperatures.

[22] In Figure 2 near Day 320 our HHMS-PI modeled pickup proton densities predicted a substantial decrease in the pickup proton densities. However, as discussed above, when we compared the HHMS-PI modeled pickup proton densities with the SWICS measured pickup proton densities we found that the SWICS measured pickup proton densities decreased even more drastically. We speculate that while this particular simulated HHMS-PI departure from the measured pickup proton densities may be due to a physical process (e.g., turbulence, stochastic acceleration) that is unaccounted for in the HHMS-PI model; it is tempting to speculate that the large shocks before Day 320, 2003 associated with the Halloween 2003 events "swept out" the neutral H in this region of the heliosphere, thus, as discussed above, reducing the production of pickup protons in this region. We look forward to revising our inflowing neutral H model so that it is mass conserving in order to determine whether the revised model would provide a more substantial decrease in the pickup proton density following the peak densities near Day 320, 2003 that is more similar to the decrease in pickup proton densities at that time measured by SWICS.

[23] We also anticipate that our future HHMS-PI simulations with various pickup proton models will help to improve general agreements between our model results and the data. That is, for example, as we change the model for the inflowing neutral H, we expect that the HHMS-PI results will improve. In the future we also plan to compare the HHMS-PI simulation results of pickup protons and their effects on IP phenomena to other available spacecraft data, including Cassini and New Horizons data obtained at greater heliocentric distances from the Sun. We also look forward to using HHMS-PI results to estimate the pickup proton parameters at Voyager 1 and Voyager 2 in the outer heliosphere.

[24] The complexity of the Halloween 2003 events and the effects of the 20 solar transients [*Detman et al.*, 2011] are quite challenging. One might inquire why we included this ambitious time interval for our first major test of HHMS-PI capabilities rather than only a quiet time interval. We had several reasons:

[25] 1. We wanted to test if the density of pickup protons would vary widely as the solar wind density and speed varied due to a major solar event.

[26] 2. We wanted to test whether shock propagation would be affected by the presence of pickup protons [*Detman et al.*, 2011].

[27] 3. We wanted to test HHMS-PI both for the background (quiet) solar wind and for an interval of major solar wind activity. There has been a great deal of interest [e.g., *Detman et al.*, 2011; *Dryer et al.*, 2004; *Intriligator et al.*, 2005a, 2005b, 2005c, 2006; 2007, 2008a, 2008b] in the Oct.–Nov. 2003 solar events at the Sun, in the inner heliosphere, and also in the outer heliosphere, including at Voyager 1 and 2.

[28] 4. We wanted to test the solar inputs for HHMS-PI for both the background mode and for the solar event mode.

[29] 5. We wanted to see if HHMS-PI could obtain the wide variations in solar wind speed, density, and temperature associated with major solar events.

[30] 6. We wanted to test if HHMS-PI could obtain the 3D global variations of solar wind parameters and shocks as the events propagated throughout the heliosphere.

[31] 7. We wanted to see the interplanetary effects of the background solar wind on the propagation of major solar events throughout the heliosphere.

[32] The results presented here gave us confidence to continue with further improvements to the model and to extend our "benchmarking" process to Cassini, and then on to Voyagers 1 and 2. We are encouraged by the agreement between the HHMS-PI simulated pickup proton densities and temperatures and the SWICS measured pickup proton densities and temperatures, and by the HHMS-PI results for SW parameters during both quiet SW and the complex Halloween 2003 events. This is our initial test of HHMS-PI for pickup protons and this relatively good agreement is an indication of the value of HHMS-PI and its robustness.

[33] We emphasize that we are using HHMS-PI to reproduce the in situ measurements that were made in 2003 for both quiet and disturbed intervals. We are not using HHMS-PI to forecast or predict interplanetary events at ACE and Ulysses. We are using HHMS-PI as a tool to simulate interplanetary observations after the fact. However, as noted above, HHMS-PI does provide the global configuration of the heliosphere at that time. It gives us the pickup proton and solar wind characteristics not just where observations were made, but everywhere from close to the Sun to the observer. This 3D heliospheric context of the specific spacecraft observations is very important for many studies. We anticipate that the use of the HHMS-PI simulations and the benchmarking of them by comparisons with spacecraft measurements will provide insights into the important input parameters and boundary conditions at the Sun as well as the significant physical processes underlying the 3D global time-dependent propagation of the quiescent and disturbed solar wind, pickup protons, the IMF, shocks, and other features throughout the heliosphere.

[34] **Acknowledgments.** The work at Carmel Research Center, Inc., was funded by NASA grant NNX08AE40G and by Carmel Research Center. We acknowledge NASA grant 44A1085637 (ACE) for supporting the analysis of the SWICS pickup ion data. We thank the NSSDC for the Ulysses SWOOPS data and for the trajectory information. We are grateful to Todd Hoeksema and the Stanford solar group and to NOAA SWPC for the solar data. We thank the reviewers for their insightful and constructive comments that led us to improving the presentation of our results.

[35] Philippa Browning thanks the reviewers for their assistance in evaluating this paper.

References

Arge, C. N., and V. J. Pizzo (2000), Improvement in the prediction of solar wind conditions using near-real time solar magnetic field updates, *J. Geophys. Res.*, *105*, 10,465–10,479, doi:10.1029/1999JA000262.

Detman, T. R., Z. Smith, M. Dryer, C. D. Fry, C. N. Arge, and V. Pizzo (2006), A hybrid heliospheric modeling system: 1. Background solar wind, *J. Geophys. Res.*, *111*, A07102, doi:10.1029/2005JA011430.

Detman, T. R., D. S. Intriligator, M. Dryer, W. Sun, C. S. Deehr, and J. Intriligator (2011), The Influence of pickup protons, from interstellar neutral hydrogen, on the propagation of the Halloween 2003 solar events to ACE and Ulysses: A 3-D MHD modelings study, *J. Geophys. Res.*, *116*, A03105, doi:10.1029/2010JA015803.

Dryer, M., Z. Smith, C. Fry, W. Sun, C. S. Deehr, and S.-I. Akasofu (2004), Real-Time predictions of interplanetary shock arrivals at L1 during the "Halloween 2003" epoch, *Space Weather*, *2*, S09001, doi:10.1029/2004SW000087.

Gloeckler, G., et al. (1992), The Solar Wind Ion Composition Spectrometer, *Astron. Astrophys. Suppl. Ser.*, *92*, 267–289.

Gloeckler, G., J. Geiss, H. Balsiger, L. A. Fisk, A. B. Galvin, F. M. Ipavich, K. W. Ogilvie, R. von Steiger, and B. Wilken (1993), Detection of interstellar pickup hydrogen in the solar system, *Science*, *261*, 70–73, doi:10.1126/science.261.5117.70.

Gloeckler, G., J. Geiss, E. Roelof, L. A. Fisk, F. Ipavich, K. Ogilvie, L. J. Lanzerotti, R. von Steiger, and B. Wilken (1994), Acceleration of interstellar pickup ions in the disturbed solar wind observed on Ulysses, *J. Geophys. Res.*, *99*, 17,637–17,643, doi:10.1029/94JA01509.

Intriligator, D. S., G. L. Siscoe, and W. D. Miller (1996), Interstellar pickup H+ ions at 8.3 AU: Pioneer 10 plasma and magnetic field analyses, *Geophys. Res. Lett.*, *23*(16), 2181–2184, doi:10.1029/96GL02052.

Intriligator, D. S., T. Detman, W. Sun, C. Fry, M. Dryer, C. Deehr, Z. Smith, and J. Intriligator (2005a), Connecting Sun and heliosphere: Proceedings of Solar Wind 11, *Eur. Space Agency Spec. Publ.*, *SP-592*, 343–346.

Intriligator, D. S., T. Detman, M. Dryer, C. Fry, W. Sun, C. Deehr, and J. Intriligator (2005b), *The Physics of Collisionless Shocks*, *AIP Conf. Proc.*, *781*, 304 pp.

Intriligator, D. S., W. Sun, M. Dryer, C. Fry, C. Deehr, and J. Intriligator (2005c), From the Sun to the outer heliosphere: Modeling and analyses of the interplanetary propagation of the October/November (Halloween) 2003 solar events, *J. Geophys. Res.*, *110*, A09S10, doi:10.1029/2004JA010939.

Intriligator, D. S., W. Sun, T. Detman, M. Dryer, C. Fry, C. Deehr, and J. Intriligator (2006), *Physics of the Inner Heliosheath*, *AIP Conf. Proc.*, *858*, 64 pp.

Intriligator, D. S., A. Rees, T. Horbury, W. Sun, T. Detman, M. Dryer, C. Deehr, and J. Intriligator (2007), *Turbulence and Nonlinear Processes in Astrophysical Plasmas*, *AIP Conf. Proc.*, *932*, 167 pp.

Intriligator, D. S., A. Rees, and T. S. Horbury (2008a), First analyses of planar magnetic structures with the Halloween 2003 events from the Earth to Voyager 1 at 93 AU, *J. Geophys. Res.*, *113*, A05102, doi:10.1029/2007JA012699.

Intriligator, D. S., W. Sun, A. Rees, T. Horbury, W. R. Webber, C. Deehr, T. Detman, M. Dryer, and J. Intriligator (2008b), *Particle Acceleration and Transport in the Heliosphere and Beyond*, *AIP Conf. Proc.*, *1039*, 375–383.

Möbius, E., D. Hovestadt, B. Klecker, M. Scholer, G. Gloeckler, and F. M. Ipavich (1985), Direct observation of He+ pick-up ions of interstellar origin in the solar wind, *Nature*, *318*, 426–429, doi:10.1038/318426a0.

Usmanov, A. V., and M. Goldstein (2006), A three-dimensional MHD solar wind model with pickup protons, *J. Geophys. Res.*, *111*, A07101, doi:10.1029/2005JA011533.

Wang, C., J. D. Richardson, and J. T. Gosling (2000), Slowdown of the solar wind in the outer heliosphere and the interstellar neutral hydrogen density, *J. Geophys. Res.*, *105*, 2337–2344, doi:10.1029/1999JA900436.

Whang, Y. C. (1998), Solar wind in the distant heliosphere, *J. Geophys. Res.*, *103*(A8), 17,419–17,428, doi:10.1029/98JA01524.